Starting Energy and Current for a Large Diameter Finite Length Backward Wave Oscillator Operated at the Fundamental Mode

K. Minami, K. Ogura, Y. Aiba, M. R. Amin, X. D. Zheng, T. Watanabe, Y. Carmel, *Senior Member, IEEE*, W. W. Destler, *Fellow, IEEE*, and V. L. Granatstein, *Fellow, IEEE*

***Abstract*—We study the starting conditions for a large diameter (diameter/wavelength = 4.8) finite length backward wave oscillator designed for 24-GHz operation at the fundamental TM_{01} mode. This geometry is very promising for high power handling capability. We analyze two separate threshold conditions. First, finite length effects give rise to a threshold in electron beam energy below which oscillations cannot be sustained at any beam current. The second is the more familiar current threshold known as a start current. It is also found that the growth rate for the fundamental mode can be much larger than those of other higher order modes thus leading to coherent operation of large diameter sources free from mode competition.**

I. Introduction

HIGH-POWER MICROWAVE sources are important for a number of advanced applications ranging from current drive and RF heating of magnetically confined plasmas in fusion devices to high resolution nanosecond radars [1]–[3]. Pulsed high power microwave oscillators utilizing intense relativistic electron beams have been extensively studied in recent years [2]–[6]. Among various microwave sources, the multiwave Cerenkov generators (MWCG's) developed by [7] at the High Current Electronics Institute, Tomsk, Russia, have recently attained record outputs [7], [8]. Radiation powers of 7.5 GW at a wavelength $\lambda = 9.7$ mm with an electronic efficiency of 20% were reported. The MWCG involves a slow wave structure (SWS) with an average diameter D much larger than λ. In the above example, $D/\lambda = 13$. This large diameter SWS enables a larger output power for a given RF energy density inside the SWS before breakdown occurs. Despite a possibility of mode competitions, efficient, high power single mode oscillation was attained in a device utilizing overmoded SWS [9]. Twenty years ago, high average power millimeter microwave sources (gyrotrons) were invented by combining an electron cyclotron maser and an overmoded open barrel cavity [2], [3]. The large diameter (overmoded) SWS in MWCG's may be an innovative key technology which corresponds to the overmoded open cavity employed in gyrotrons, although the final evaluation of performance and the feasibility of using MWCG's in actual applications are yet to be established. The MWCG has a close relationship to conventional backward wave oscillators (BWO's), since both employ SWS's in common [4], [5], [7]–[14].

Although the physical processes involved in the MWCG's [7], [8] are complicated, we point out here that high-power millimeter microwaves can be generated without decreasing the mean diameter of the SWS. Both BWO's and large diameter BWO's can be operated in the fundamental TM_{01} mode as will be shown in this paper. The difference in SWS's between the two devices is as follows. The inner radius of the metal surface of the SWS, $R(z)$, is assumed to vary sinusoidally around the mean radius R_0, i.e., $R(z) = R_0 + h \cos K_0 z$, $K_0 = 2\pi/z_0$. Here, z_0 and h are, respectively, the axial length of periodicity and the amplitude of corrugation. In BWO's [4], [5], [10]–[14], the mean radii, $R_0 = D/2$, were chosen such that $D/\lambda = 2R_0/\lambda \sim 1$, whereas, in the present large diameter BWO, the condition $D/\lambda \gg 1$ is explored. The key point is that, in the latter, oscillation frequency is raised by carefully choosing small values of h and z_0, keeping R_0 larger than λ. This situation is quite similar to the SWS design of MWCG's [7]–[9]. In the present paper, numerical studies are made within the scope of linear analysis for a large diameter SWS with $D/\lambda \sim 4.8$. Specifically, the starting energy and the starting current of the beams for initiating microwave oscillation in such a finite length SWS are analyzed in detail. Previously, the starting current conditions for finite length BWO's have been studied by various authors [5], [13], [15], [16]. Swegle analyzed the starting condition for a BWO [15]. In his treatment, 100% reflection at the beam entrance boundary and 0% reflection at the RF output boundary were assumed. This assumption was valid for the case of matched termination at the output end of the SWS. We consider here an alternative case of nonzero round trip reflection which may correspond to the experimental situations in [4] and [10]. Such nonzero round trip reflection produces discrete spectra of axial wavenumber of eigenmodes of an axisymmetric TM mode [13], [14], [17].

In Section II, we describe the model of our linear analysis. The difficulties to be overcome in the practical numerical computation in the case of $D/\lambda \gg 1$ are discussed. Numerical results are shown in Section III. Discussion and conclusions are given in Section IV.

Manuscript received April 8, 1994; revised December 19, 1994.

K. Minami, K. Ogura, Y. Aiba, M. R. Amin, and X. D. Zheng are with the Graduate School of Science and Technology, Niigata University, Niigata City, 950-21, Japan.

T. Watanabe is with National Institute for Fusion Science, Nagoya 464-01, Japan.

Y. Carmel, W. W. Destler, and V. L. Granatstein are with the Institute for Plasma Research, University of Maryland, College Park, MD 20742 USA.

IEEE Log Number 9409799.

II. Formulation and Difficulties in Numerical Analysis

The model of an axisymmetric large diameter SWS with length L shown in Fig. 1 is analyzed. The radius $R(z)$ of perfectly conducting metal wall varies with $R(z) = R_0 + h\cos K_0 z$. The entire system is immersed in a strong longitudinal external magnetic field. The transverse motion of the beam electrons is assumed to be negligible. We also assume that an infinitely thin annular beam with radius R_b, monoenergetic beam energy V_b and current I_b is incident to the SWS. The linear dispersion relation for the system in Fig. 1 was derived previously [15], [18], [19] and the results are summarized here. The boundary condition that the tangential components of the RF electric field at the corrugated metal surface of the SWS must be zero gives

$$\sum_{m,\ n=-\infty}^{\infty} [1+(n-m)Q_n](B_n C^J_{mn} + C_n C^N_{mn}) = D_{mn}\cdot A_n = 0 \tag{1}$$

$$C^J_{mn} = \int_{-\pi/K_0}^{\pi/K_0} \exp\,[i(n-m)K_0 z] \cdot J_0[y_n(1+\alpha\ \cos\ K_0 z)]\,dz \tag{2}$$

$$= \sum_{q=0}^{\infty} \frac{(y_n\alpha)^{(2q+|n-m|)} J_0^{(2q+|n-m|)}(y_n)}{2^{2q+|n-m|} q!(q+|n-m|)!},$$

$$\alpha = h/R_0 \tag{3}$$

where $Q_n = K_0 k_n/(\omega^2/c^2 - k_n^2)$, $k_n = k + nK_0$, $y_n^2 = R_0^2(\omega^2/c^2 - k_n^2)$ and c is the vacuum velocity of light. The RF field amplitudes, A_n, B_n, and C_n of the Floquet harmonics are the same as those in (7) in [18]. The beam quantities such as I_b and V_b are involved in B_n and C_n. In (1), C^N_{mn} is obtained by replacing the Bessel function of the first kind, J_0, in C^J_{mn} by that of the second kind, N_0. In the above expressions, temporal and spatial phase factors $\exp\,[i(k_n z - \omega t)]$ have been assumed for every RF quantity. The dispersion relation combining ω and k is given from (1) as the determinant equation,

$$D(k,\ \omega) = \det\,[D_{mn}] = 0 \tag{4}$$

which is required to have nontrivial A_n in (1). As is well known, N_0 goes to infinity at the origin which occurs in the case of light line in vacuum, $\omega = ck_n$. Because the roots of (4) are slow waves, they are located in the complex ω and k planes considerably separated from where $\omega = ck_n$. Difficulty of N_0 infinity does not occur for finding the roots.

We discuss here some peculiar difficulties that arise in the computation for the large diameter SWS. For the time being, we consider the simple case without the beam, i.e., $I_b = 0$, and $A_n = B_n$, $C_n = 0$ in (1) accordingly [18]. Because no input energy is present in the SWS, oscillations cannot be expected. For a real ω, real k's are obtained in (4) and vice versa. Equations (2) and (3) were useful to compute the dispersion relation of a BWO [19], [20]. In the present case of large diameter BWO's, however, there exist some difficulties for computing (2) and (3). In order to get a large oscillation frequency $\omega/2\pi$ without decreasing R_0, we must choose a small h and z_0 in Fig. 1 that results in a large K_0 and that makes $y_n^2 < 0$ in (2). For negative y_n^2, the Bessel function J_0 becomes modified Bessel function I_0 consequently, and the integrand of (2) is rewritten as $\exp\,[i(n-m)K_0 z] I_0[y'_n(1+\alpha\ \cos\ K_0 z)]$, where $y_n^2 = -y_n'^2$. The modified Bessel function I_0 in the integrand becomes extremely large, if y'_n is large. This effect causes an overflow in the process of numerical computation of (4). Such a difficulty arises often in the calculation of the large diameter SWS with small z_0. To avoid the difficulty, we express $I_\nu(z)$ as

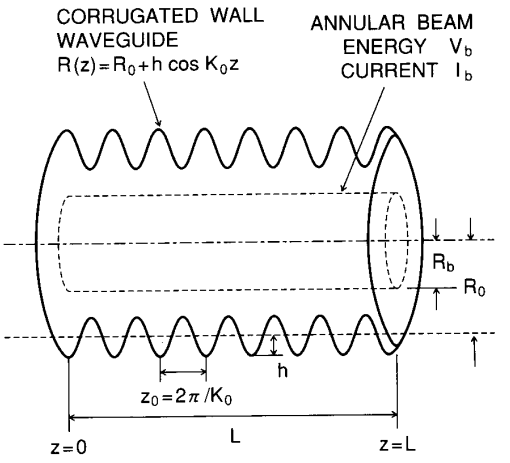

Fig. 1. Model of analysis. Annular beam of monochromatic energy V_b and current I_b is incident on the axisymmetric corrugated wall large diameter slow wave structure with length L.

$$I_\nu = \frac{e^z}{(2\pi z)^{1/2}}\left(1 - \frac{\mu-1}{8z} + \frac{(\mu-1)(\mu-9)}{2!(8z)^2} - \cdots\right)$$
$$|\arg\,(z)| < \frac{\pi}{2}, \qquad \mu = 4\nu^2.$$

Using this asymptotic expansion, (1) is expressed as

$$\sum_{m,\ n=-\infty}^{\infty} [1+(n-m)Q_n]\,\frac{C^J_{mn}}{\exp\,(y'_n)}\,G_n = D'_{mn}\cdot G_n$$
$$G_n = A_n\ \exp\,(y'_n),$$
$$D'(k,\ \omega) = \det\,[D'_{mn}] = 0. \tag{5}$$

The dispersion relation is given by (5) instead of (4). Equation (5) does not have problems with numerical overflow.

The next problem concerns the adequacy of the Taylor expansion used in (3). In general, numerical integration of (2) takes much computation time and the expanded form of (3) is preferable, as long as the sinusoidally corrugated SWS in Fig. 1 is considered. A large K_0 again may result in $|y_n\alpha| > 1$ in (3), and the summation does not converge rapidly. We find that tens of terms in (3) must be calculated to get a converged value of summation because of increased denominators. To avoid this difficulty, we truncate the rank of the determinant in (5) to as small a value as possible. This is because the values of k_n and accordingly y_n will not be very large for small

ranks of truncated determinant. For example, $|y_n\alpha| \gg 1$ may be avoided, if one limits $-1 \leq n,\ m \leq 0$ (2×2 determinant) or $-1 \leq n,\ m \leq 1$ (3×3 determinant). Fig. 2 shows the result of the design study; the oscillation frequency $f = \omega/2\pi$ versus the corrugation wavenumber K_0 for several corrugation amplitudes h. Here, $R_0 = 3.0$ cm has been assumed as a given parameter. Curves in the figure are obtained by computing the frequencies at the crossing point of the structure mode and the beam space charge line with $I_b = 0$ for various values of K_0 and h. The straight line, $\omega = V_b K_0/2$, in Fig. 2 is the boundary that divides the BWO (absolute instability) from the TWT (convective instability) for the case of π-mode operation ($k = K_0/2$) with $V_b = 100$ keV. Microwave oscillation can be expected in the cases of K_0 to the left of the straight boundary line. Roughly speaking, BWO's and large diameter BWO's are expected, respectively, in cases of $K_0 < 10$ cm^{-1} and $K_0 > 10$ cm^{-1}. The black circle represents the parameters we have chosen for the present design study of a large diameter BWO with the following parameters: $K_0 = 18.5$ cm^{-1} ($z_0 = 0.34$ cm), $h = 0.17$ cm and $f = 24$ GHz. The solid and dashed curves are, respectively, the calculations using (3) and (5) of the 9×9 and 2×2 approximate truncated determinants. The differences between both curves are less than 4%. For the chosen size parameters, the dispersion curves are calculated for various truncated ranks from 9 (9×9) to 2 (2×2) of the determinant in (5). For ranks larger than 6, the oscillation frequencies are almost unchanged, and the results are considered to be exact. Even in the case of rank 2, the deviations from exact values are less than several percent. These facts suggest that the truncation to the rank 2 of the determinant in (5) is almost correct for our purpose. Hence, in order to save computation time, we adopt the truncated determinant of rank 2 in the subsequent numerical analysis of complex ω and k with incident beams, at the sacrifice of accuracy within a few percent.

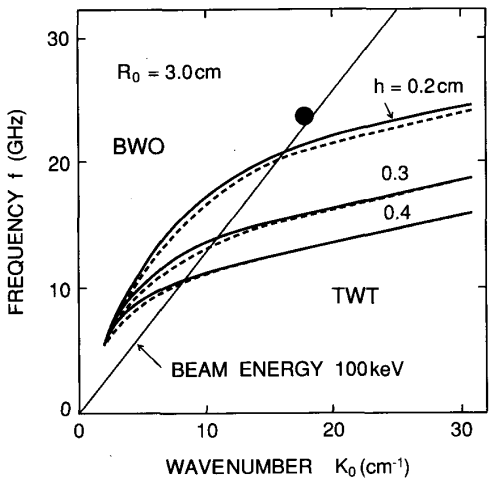

Fig. 2. Design study of the slow wave structure. Oscillation frequency for 100 keV beam versus corrugation wavenumber K_0 for various corrugation amplitudes h. The mean radius is $R_0 = 3.0$ cm. The solid and dashed curves are, respectively, 9×9 and 2×2 approximate results of the determinant of the dispersion relation. The black circle is the chosen parameters of our large diameter backward wave oscillator.

III. Numerical Results

A. Infinitely Long Slow Wave Structure

The parameters of the large diameter SWS used in the following numerical analysis are: $R_0 = 3.0$, $h = 0.17$, $z_0 = 0.34$, and $R_b = 2.63$ cm. Beam energies of $V_b = 100$ and 65 keV are used as typical values. The beam current I_b is mostly assumed to be 0.4 kA, unless specified otherwise.

The dispersion relation (5) for complex $\omega/2\pi$ versus real wavenumber k is shown in Fig. 3 for two values of V_b, 100 and 65 keV represented, respectively, by solid and dashed curves. Real and imaginary parts of $\omega/2\pi$ are shown, respectively, in (a) and (b). Here, the beam current of $I_b = 0.4$ kA has been assumed. Because of Floquet's theorem, the dispersion curves have periodicity K_0 for wavenumber k, in other words, $\omega(k) = \omega(k + nK_0)$. Usually, figures are shown for the first Brillouin zone $-K_0/2 \leq k \leq K_0/2$, however, we depict hereafter the curves for $0 \leq k \leq K_0$, because the important parts of the curves are located near $k = K_0/2$. As were pointed out previously, there exist generally 4 independent roots for the fundamental TM_{01} mode [18], [20]. They are the fast and slow space charge waves and the backward and forward structure waves. The first wave is always heavily damped and it is ignored entirely in the subsequent analysis. The second wave is the energy source for the third wave, i.e., the output radiation. The fourth wave can serve as a positive feedback mechanism in the case of a finite length SWS. For simplicity, the fourth wave is also ignored hereafter. For a real k, (5) can have a pair of complex conjugate roots of ω. They are a growing slow space charge wave and a decaying fast space charge wave. The single beam line for infinitesimal currents is split into the fast (shown by F) and slow (shown by S) beam space charge waves in Fig. 3(a), because of nonzero beam current. Absolute instability can be found around the crossing point of the backward structure wave (shown by B) and the line S. It is noted in Fig. 3 that the ranges of k for instability, i.e., complex ω shown by thick solid and dashed lines in Fig. 3(b), are much more limited than the previous case of BWO's [18], [19]. This is because the corrugation parameter $\alpha = h/R_0$ is presently smaller than those in the conventional BWO's. In other words, the oscillation condition in large diameter BWO's with $D/\lambda \gg 1$ is more restrictive or stringent than those in BWO's with $D/\lambda \sim 1$.

In our large diameter (overmoded) SWS, there exists a possibility of mode competition between various candidates including the fundamental and higher modes. Steady oscillation of the fundamental mode may not be realized because the beam energy may be fed to various modes with higher frequencies. In order to clarify the situation, we extended the analysis for the fundamental mode shown in Fig. 3 up to sixth higher modes. The oscillation frequency and the maximum temporal growth rate of the fundamental TM_{01} mode are compared with those of higher modes. We computed the dispersion curves similar to Fig. 3 for each higher mode. Fig. 4 shows the dispersion curves for an infinitesimal beam current,

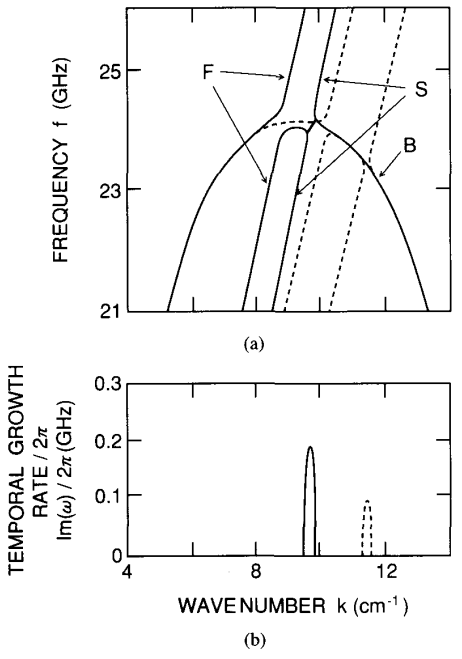

Fig. 3. Dispersion relation for complex $\omega/2\pi$ versus real wavenumber k. $I_b = 0.4$ kA. Solid curves are for $V_b = 100$ keV and dashed curves are for $V_b = 65$ keV. (a) $f = \mathrm{Re}\ (\omega)/2\pi$ versus k. (b) $I_m(\omega)/2\pi$ versus k.

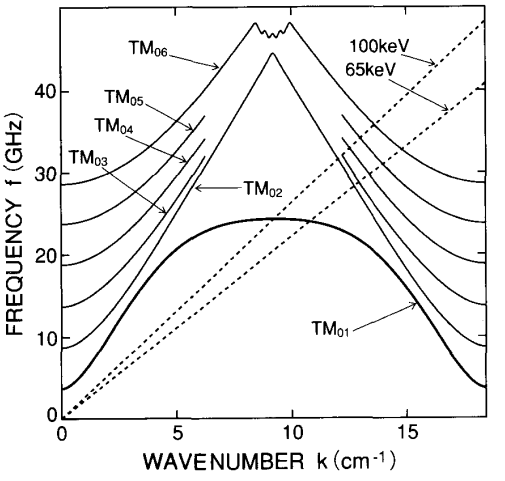

Fig. 4. The dispersion curves for TM_{01}, $\cdots$, TM_{06} modes. The two dashed lines are the beam lines for 100 and 65 keV with infinitesimal currents, respectively. The crossing points of the beam lines and structure curves give possible oscillation frequencies.

TABLE I
COMPARISON OF OSCILLATION OF SIX MODES INCLUDING THE FUNDAMENTAL TM_{01} MODE. THE OSCILLATION WAVENUMBER AND FREQUENCY AT THE MAXIMUM TEMPORAL GROWTH RATE ARE LISTED FOR OUR DESIGNED LARGE DIAMETER SLOW WAVE STRUCTURE. BEAM ENERGY AND CURRENT ARE, RESPECTIVELY 100 KEV AND 0.5KA

Mode	Oscillation Wavenumber (cm-1)	Oscillation Frequency (GHz)	Maximum Temporal Growth Rate (rad/ns)
TM_{01}	9.8	24.1	0.195
TM_{02}	12.3	30.4	0.0048
TM_{03}	12.5	30.9	0.0118
TM_{04}	12.8	31.8	0.0142
TM_{05}	13.3	33.1	0.0132
TM_{06}	14.0	34.8	0.0132

from which the oscillation frequencies can be estimated. It is interesting to note that the dashed beam lines, 100 and 65 keV, intersect the curve of the fundamental TM_{01} mode at the positions where the group velocities are much smaller than those for higher modes. The results from complex analysis like Fig. 3 are summarized in Table I, where the maximum temporal growth rate, corresponding oscillation frequency and oscillation wavenumber are listed for six modes. Here, the beam current 0.5 kA has been assumed. As is clearly shown in the table, the maximum temporal growth rates of the higher modes are much smaller than that of the fundamental TM_{01} mode. Accordingly, oscillations of higher modes may be ignored in the scope of the present linear analysis. Of course, mode competitions may be expected in large diameter BWO's at the saturated level of oscillation in general. At the linear stage, however, mode competitions are insignificant in the large diameter SWS, if the size and beam parameters are carefully chosen. For this reason, we limit ourselves the subsequent analysis to the fundamental TM_{01} mode.

The dashed curves in Fig. 3 are for the case of $V_b = 65$ keV. The temporal growth rate $\mathrm{Im}\ (\omega)$ for $V_b = 65$ keV shown by the dashed curve in Fig. 3(b) is considerably smaller than that for $V_b = 100$ keV shown by the solid curve. This difference suggests that, like conventional BWO's, there exists a starting energy threshold for oscillation in a finite length large diameter SWS as will be analyzed in the next subsection.

In Fig. 3, the real wavenumber k has been assumed. The real k means that we have assumed a sinusoidal small origin of oscillation with infinite extent in the z direction and have calculated its temporal evolution. On the other hand, in the case of a localized small origin of disturbance for the instability, the origin develops asymptotically with temporal and spatial factors $t^{-1/2}\ \exp\ [-i(\omega_s t - k_s z)]$, as was shown in (2.22) in [21]. Here, ω_s and k_s are, respectively, the complex angular frequency and complex wavenumber at the saddle point $\partial\omega_s/\partial k_s = 0$ in (5). The localized origin can monotonically grow up in time at every point in z. This is therefore an absolute instability. Once an unstable root of (5) in Fig. 3 is found, it is not very difficult to access the saddle point, ω_s and k_s, which exists uniquely for a given set of all parameters, by using the Newton–Raphson technique. In the saddle point analysis of the large diameter BWO, it is found that the oscillation frequency $\mathrm{Re}\ (\omega_s)/2\pi$ and the temporal growth rate $\mathrm{Im}\ (\omega_s)$ are, respectively, slightly decreasing and increasing functions of I_b, and the spatial growth rate $\mathrm{Im}\ (k_s)$ is almost unchanged with increase in I_b.

B. Finite Length Slow Wave Structure

In a large diameter SWS with finite length L as shown in Fig. 1, the wave reflections (or leakages) at both ends are taken into account. The end reflections result in a feedback mechanism by the backward structure wave, and the distinc-

tion between absolute and convective instabilities becomes somewhat ambiguous in the L finite case. The complex wavenumbers of the slow space charge wave and the backward structure wave are denoted, respectively, by a_+ and a_-. In the limit of infinite L, a_+ $(= a_-)$ coincides with the saddle point of (5). For L finite cases, the following equations must be satisfied instead of (5), [20].

$$D(a_+, \omega) = 0 \tag{6}$$

$$D(a_-, \omega) = 0 \tag{7}$$

$$R \exp\left[-i(a_- - a_+)L\right] = 1. \tag{8}$$

Equation (8) comes from the requirement that the electromagnetic field must be a single value at every z point, when the propagating wave comes back after one round trip [20]. In (8), R is the one round trip reflection coefficient of wave fields at the both ends of the SWS, and assumed to be a given parameter. The length L is assumed to be $L = 70z_0 = 23.8$ cm. In general, the reflection coefficient R in (8) must be a complex number, however, for simplicity it is approximately replaced by a real number $0 < R < 1$ in the subsequent analysis. This is because the argument of the complex number causes only changes in equivalent structure length less than z_0 much smaller than L. The additional requirement given by (8) results in the existence of the starting energy in addition to a nonzero starting current in finite L BWO's. Equation (8) is rewritten as

$$\text{Re}\,(a_- - a_+) = -2\pi N/L > 0 \tag{9}$$

$$\text{Im}\,(a_- - a_+) = -\ln(R)/L > 0 \tag{10}$$

where N is an integer. The following analysis is limited to the case $N = -1$ in (9), because $N = -1$ is the easiest case for initiating oscillation among various choices of N for a given L.

To solve (6)–(8) correctly, it is necessary to watch the movements of roots a_+ and a_- on the complex k plane for various ω's with positive Im (ω) approaching to zero [20], [21]. This is because the physical meaning (stable or unstable) of the each root is lost in the course of numerical calculation of (6)–(8). We must reconsider the physical meaning through watching the movement of the root on the complex k plane. If the particular root traverses the real axis during the change in Im (ω) from a large positive number to zero, the root is unstable, otherwise it is stable. A pair of solutions a_+ and a_- is shown on the complex k plane in Fig. 5(a) for the case of $V_b = 100$ keV. The locations of the roots a_+ and a_- are found at the centers of the contour mapping of $|D'|$ given by (6)–(8) on the complex k plane. The corresponding common value of complex $\omega/2\pi = 24.103 + i0.063$ is found in Fig. 5(b) for both a_+ and a_- shown by black circles on the same complex k plane as Fig 5(a). The white circles in Fig. 5(b) are the locations of Im $(\omega) = 0$ that give the boundary lines between BWO's (Im $(\omega) > 0$), and TWT's (Im $(\omega) < 0$). The arrows on the solid lines show the directions of decrease in Im $(\omega)/2\pi$ toward zero for constant Re $(\omega)/2\pi$. The diamond is the saddle point of (5). In L infinite case, oscillation (absolute instability) is expected at the saddle point as was stated in the previous subsection, if it is located in Im $(\omega) \geq 0$ region in complex k plane. In this case, oscillation is expected even for infinitesimal beam currents and no limitations exist for starting energy. In L finite case, however, the oscillation happens not at the saddle point but at a_+ obtained from (6)–(8). Oscillation is impossible, if the pair of the roots are located in Im $(\omega) \leq 0$ region. Because the black circles are located in the region Im $(\omega) > 0$ in Fig. 5(b), the oscillation can be expected in the present case of $V_b = 100$ keV. Since we have chosen $L = 23.8$ cm and $N = -1$, Re $(a_- - a_+) = 0.264$ cm^{-1} from (9) is a fixed value, which is independent of the value of reflection coefficient R. The horizontal distance between a_+ and a_- is a constant 0.264 cm^{-1} on the complex k plane shown in Fig. 5(b).

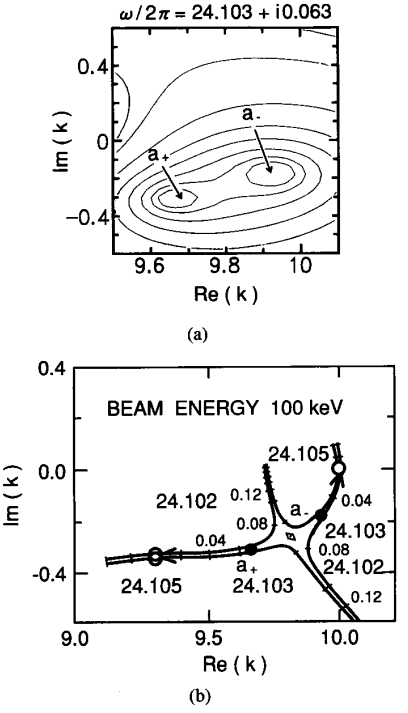

Fig. 5. Locations of the pair of roots, a_+ and a_-, on the complex k plane for $V_b = 100$ keV and $I_b = 0.4$ kA, $L = 23.8$ cm, $N = -1$ and $\omega/2\pi = 24.103 + i0.063$. (a) Contour mapping of $|D|$ where D is defined by (5). (b) Locations of the roots (black circles) that are in the oscillation region within border lines of Im$(\omega) \geq 0$ shown by white circles. The diamond is the saddle point.

A pair of solutions a_+ and a_- in (6)–(8) in the case of $V_b = 65$ keV is shown on the complex k plane in Fig. 6. Other parameters are the same as those in Fig. 5. The corresponding common value of complex $\omega/2\pi = 23.295 - i0.092$ is found in Fig. 6 for both a_+ and a_- shown by black circles. In this case, a_+ and a_- are located in the region of TWT's, Im $(\omega) < 0$, and oscillation cannot occur for $V_b = 65$ keV, although the beam current $I_b = 0.4$ kA is identical to that for $V_b = 100$ keV in Fig. 5. Comparing Figs. 5(b) and 6, one finds that there may exist a threshold value in the beam energy V_b below which oscillation in the BWO's stops, no matter how

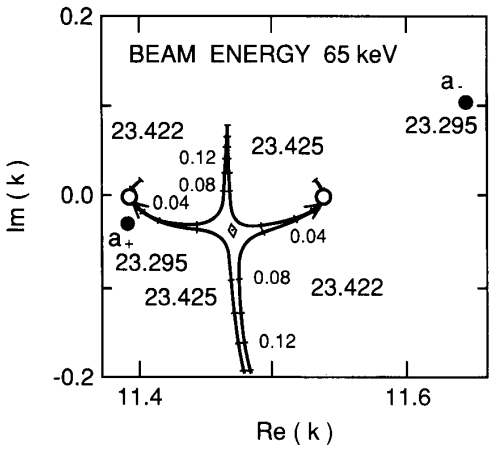

Fig. 6. Locations of the pair of roots, a_+ and a_-, on the complex k plane for $V_b = 65$ keV and $I_b = 0.4$ kA, $L = 23.8$ cm, $N = -1$ and $\omega/2\pi = 23.295 - i0.092$. Locations of the roots (black circles) are outside the oscillation region Im $(\omega) \geq 0$ shown by white circles. The diamond is the saddle point.

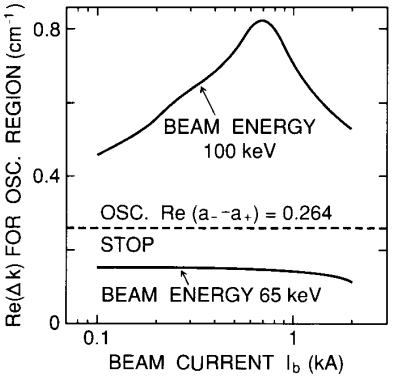

Fig. 7. Allowable oscillation regions of two solid curves for $V_b = 100$ and 65 keV, i.e., horizontal separation of open circles as shown in Figs. 5(b) and 6 versus beam current I_b. The dashed line is the horizontal separation Re $(a_- - a_+) = 0.264$ cm^{-1} of the roots for $I_b = 0.4$ kA, $L = 23.8$ cm, and$N = -1$ in (9).

large the beam current I_b. This statement is clarified in Fig. 7, where the fixed horizontal separation between two black circles Re $(a_- - a_+) = 0.264$ cm^{-1} given from (9) is shown by a horizontal dashed line. Two solid curves are the horizontal separations Re (Δk) between two white circles, respectively, as shown in Figs. 5(b) and 6 as functions of I_b. Here, Re (Δk) is the allowable range of oscillation for a given I_b. In the case

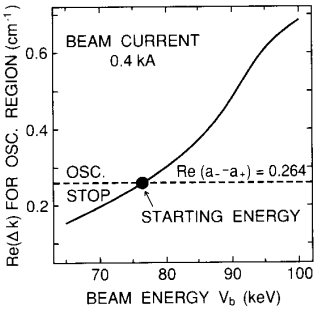

Fig. 8. Oscillation region versus beam energy V_b. The dashed line is the horizontal separation Re $(a_- - a_+) = 0.264$ cm^{-1} for $I_b = 0.4$ kA, $L = 23.8$ cm, and $N = -1$. The black circle is the starting energy.

of $V_b = 100$ keV, the solid curve always lies above the dashed line. This fact suggests that the oscillation is possible. On the other hand, in the case of $V_b = 65$ keV, the curve stays below the dashed line, and oscillation does not occur.

For a given current $I_b = 0.4$ kA, the starting energy for oscillation is found in Fig. 8, where the horizontal separations Re (Δk) of white circles such as those in Fig. 5(b) or 6 versus V_b are plotted. It is clearly shown that the starting energy denoted by the black circle is 76.5 keV for the given parameters of the present large diameter SWS. The larger length L, the smaller starting energy, because the dashed line becomes lower. It must be emphasized, however, that the starting energy is not a sufficient condition, but a necessary condition for initiating oscillation in the finite length SWS. In order to have oscillation, the pair of roots a_+ and a_- must also satisfy (10) in addition to (9). This additional condition yields the starting current for oscillation. Equation (10) includes the reflection coefficient R as a given parameter, and the starting current I_{st} is affected sensitively by R. The results are shown in Fig. 9, where I_{st} versus R is calculated for $V_b = 100$ keV and $L = 23.8$ cm. It is reasonably shown that I_{st} is a decreasing function of R. If we take into account the effect of the fourth wave (forward structure wave) as an additional feedback mechanism in (8), an oscillatory nature arises in the curve I_{st} versus L, as was pointed out in [13], [16].

IV. Discussion and Conclusions

A large diameter backward wave oscillator of $D/\lambda \sim 4.8$ has been designed and analyzed numerically in detail. The key point of the design study is to raise the oscillation frequency without decreasing the mean diameter of the SWS. In our linear analysis, parameter selection for such purposes has been readily performed.

It was shown in the previous section that there existed a starting current of the beam required to withstand the leakage of radiation at both ends of SWS. Moreover, there existed a starting energy of the incident beam, below which oscillation could not occur, because of the finite length of the SWS. These two statements are never trivial and the distinction between both conditions has not been clarified in the literatures in the past. The former condition for the starting current given

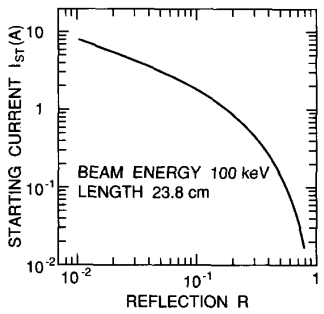

Fig. 9. Starting current I_{st} versus reflection coefficient R for beam energy $V_b = 100$ keV, $L = 23.8$ cm, and $N = -1$.

by (10) arises from the requirement that the radiation loss depending on I_b at the ends of the SWS must be smaller than a threshold value. In other words, the external Q value of the corrugated wall resonator shown in Fig. 1 must be large enough for the occurrence of oscillations. The resonator must store a minimum amount of RF energy for oscillation. On the other hand, the latter condition for the starting energy given by (9) arises from the requirement that the coupling condition of real wavenumbers, Re (a_+) and Re (a_-), between the donor of RF energy a_+ (slow space charge wave) and the acceptor a_- (backward structure wave) becomes stringent, when L is small. The locations of the a_+ and a_- on the complex k plane are considerably separated in relatively short L case, and the coupling condition, namely, phase matching condition of the waves at the ends may not be satisfied. This restriction, Re (Δk), is relaxed in the case of large V_b as was shown in Fig. 8. This is the reason for the existence of the minimum starting energy for oscillation. This oscillation condition for V_b is peculiar to the finite L case, and such additional requirement for the coupling of waves did not occur in conventional infinite L case shown in Fig. 3. It is well known that beam wave interaction is strong near π or 2π mode operation, where the group velocity of the backward structure wave is small. In L finite case, the oscillation may stop somewhere between two mode operations because of increased group velocity. This qualitatively well known fact is for the first time analyzed quantitatively in the present paper, and it is the significance of the starting energy analyzed in this paper.

The diffraction of the radiation at the ends of large diameter SWS relating the value of reflection coefficient R is a complicated problem to analyze, and it is not treated here. In our numerical analysis, $L = 23.8$, $R_0 = 3.0$, and $\lambda = 1.25$ cm. The structure length L may be considered to be longer enough than R_0 and λ, and our analysis ignoring end diffraction problem may be qualitatively valid. The practical value of the reflection coefficient R of the large diameter SWS can be measured by means of vector network analyzers for a real fabricated sample. The coefficient R is estimated to be 0.2 at 20 GHz from a straight cylindrical waveguide assuming that the corrugation parameter $\alpha = h/R_0 = 0.0567$ is small enough. Then, the starting current $I_{st} = 1$ A is found in Fig. 9. In the previous section, we assumed the typical beam current $I_b = 0.4$ kA, which is 400 times larger than I_{st}. In such cases, overbunch instability may occur in the oscillation and degradation of the microwave output may result as was predicted and observed in [5] and [13]. In order to suppress the instability, we may raise I_{st} by decreasing the length L under the restriction that the pair of roots in (9) remain in the oscillation region shown in Fig. 5(b). On the other hand, space charge limiting current in a cylindrical pipe for the average radius $R_0 = 3$ cm and beam radius $R_b = 2.68$ cm is calculated to be $17(\gamma^{2/3} - 1)^{3/2}/2 \ln (R_b/R_0) = 2.9$ kA, which is much larger than the present I_b, where γ is the relativistic factor. The nonlinear analysis [22] or numerical simulation [13] is required to predict the power level and the performances of the designed large diameter BWO.

The energy sources in gyrotrons are the beam velocity$v_\perp$ perpendicular to the axial magnetic field. Electron beams with $v_\perp/v_{||} = 1.5 \sim 2$ are usually required for high efficiency operation in gyrotrons [2], [3]. For that purpose, a sophisticated technology to generate such spiral beams was devised by means of magnetron injection gun, and analytically and empirically adjusted nonuniform axial magnetic field profiles for optimized performance. In contrast to gyrotrons, BWO's are easy to operate, because beams with $v_\perp/v_{||} \ll 1$ are available, and uniform axial magnetic fields are usually applicable.

The growth rates of the large diameter BWO analyzed in the present paper are smaller than those in the conventional BWO's. This is mainly because we have chosen small $\alpha = h/R_0$. In fact, we carried out a preliminary measurement of BWO operation of our designed large diameter SWS. It was found that the microwave output at 21 GHz was quite small and that the operation was made in linear regime. It may be important to explore a possibility of enhancing the growth rates of radiation from the large diameter BWO. Our analysis has been confined to the case of very strong applied magnetic field. An extension of the present linear analysis to the finite magnetic field case, especially the case $\omega \sim \Omega$, is very important [6]. Here, Ω is the relativistic electron cyclotron frequency.

Reference [23] pointed out that, in slow wave cyclotron devices with $v_{||} < \omega/k < c$, the beam energy can be converted to wave energy through a transformation from $v_{||}$ to $v_\perp$. This device was called the slow wave electron cyclotron maser. Although they assumed a dielectric loaded smooth cylindrical configuration, their statement can be applied to a metal wall SWS [24], [25]. In fast wave devices such as gyrotrons, the normal Doppler shifted beam cyclotron wave, $\omega = kv_{||} + \Omega$, is used to interact with structure TE modes. On the other hand, the anomalous Doppler shifted beam cyclotron wave, $\omega = kv_{||} - \Omega$, may be available to interact with structure TM modes in our large diameter SWS. The growth rates in the large diameter BWO in the present paper may be resonantly enhanced by the novel effect suggested by Kho and Lin [23]. Moreover, they showed in their Fig. 6 that the slow wave electron cyclotron maser was more tolerant of beam momentum spread than a fast wave device (CARM) for high efficiency operation. Their results are especially encouraging in the case of high beam current in which beam qualities such

as momentum spread and emittance are greatly inferior to the beams generated from thermoionic cathodes [26].

In conclusion, the slow wave devices such as MWCG's will be a hopeful candidate for the purpose of generating multi-MW millimeter microwaves for a variety of advanced applications. The large diameter BWO studied in the present paper may be helpful for that purpose.

REFERENCES

[1] A. V. L. Gaponov-Grekhov and V. L. Granatstein, Ed., *High Power Microwave Applications for the 21st Century.* Dedham, MA: Artech House, 1994.

[2] V. L. Granatstein and I. Alexeff, Ed., *High-Power Microwave Sources.* Dedham, MA: Artech House, 1987.

[3] J. N. Benford and J. A. Swegle, *High Power Microwaves.* Boston, MA: Artech, 1992.

[4] R. A. Kehs *et al.*, "A high power backward-wave oscillator driven by a relativistic electron beam," *IEEE Trans. Plasma Sci.*, vol. PS-13, pp. 559–562, Dec. 1985.

[5] Y. Carmel *et al.*, "From linearity toward chaos: Basic studies of relativistic backward-wave oscillators," *Phys. Rev. Lett.*, vol. 69, no. 11, pp. 1652–1655, Sept. 1992.

[6] A. Vlasov *et al.*, "Relativistic backward-wave oscillators operating near cyclotron resonance," *Phys. Fluids B*, vol. 5, no. 5, pp. 1625–1638, May 1993.

[7] S. P. Bugaev *et al.*, "Investigation of a millimeter-wavelength-range relativistic diffraction generator," *IEEE Trans. Plasma Sci.*, vol. 18, pp. 518–524, June 1990.

[8] ——, "Relativistic multiwave Cerenkov generators," *IEEE Trans. Plasma Sci.*, vol. 18, pp. 525–536, June 1990.

[9] D. K. Abe, "Experimental studies of overmoded high power microwave generators," Ph.D. dissertation, Univ. Maryland, College Park, 1992.

[10] Y. Carmel *et al.*, "High-power microwave generation by excitation of a plasma-filled rippled boundary resonator," *IEEE Trans. Plasma Sci.*, vol. 18, pp. 497–506, June 1990.

[11] X. Zhai *et al.*, "Observation of Trivelpiece-Gould modes in a plasma filled backward wave oscillator," *Phys. Rev. A*, vol. 45, no. 12 , pp. R8336–R8339, June 1992.

[12] J. A. Swegle *et al.*, "Scaling studies and time-resolved microwave measurements on a relativistic backward-wave oscillator," *IEEE Trans. Plasma Sci.*, vol. 21, pp. 714–724, Dec. 1993.

[13] B. Levush *et al.*, "Theory of relativistic backward-wave oscillators with end reflections," *IEEE Trans. Plasma Sci.*, vol. 20, pp. 263–280, June 1992.

[14] Y. Carmel *et al.*, "Relativistic plasma microwave electronics: Studies of high-power plasma-filled backward-wave oscillators," *Phys. Fluids B*, vol. 4, no. 7, pp. 2286–2292, July 1992.

[15] J. A. Swegle, "Starting conditions for relativistic backward wave oscillators at low currents," *Phys. Fluids*, vol. 30. no. 4, pp. 1201–1211, Apr. 1987.

[16] K. Minami *et al.*, "Analysis of starting currents in a backward wave oscillator with finite structure length," *J. Phys. Soc. Jpn.*, vol. 61, no. 10, pp. 3566–3575, Oct. 1992.

[17] M. R. Amin *et al.*, "Analysis of the electromagnetic waves in an overmoded finite length slow wave structure," *IEEE Trans. Microwave Theory Tech.*, vol. 43, Apr. 1995.

[18] J. A. Swegle *et al.*, "Backward wave oscillators with rippled wall resonators: Analytic theory and numerical simulation," *Phys. Fluids*, vol. 28, no. 9, pp. 2882–2894, Sept. 1985.

[19] K. Minami *et al.*, "Linear theory of electromagnetic wave generation in a plasma-loaded corrugated-wall resonator," *IEEE Trans. Plasma Sci.*, vol. 18, pp. 537–545, June 1990.

[20] M. M. Ali *et al.*, "Linear analysis of a finite length plasma-filled backward wave oscillators," *Phys. Fluids B*, vol. 4, no. 4, pp. 1023–1032, Apr. 1992.

[21] R. J. Briggs, *Electron-Stream Interaction with Plasmas.* Cambridge, MA: MIT Press, 1964.

[22] T. Watanabe *et al.*, "Effect of beam energy spread on radiation intensity in a high-power backward wave oscillator with finite length," *J. Phys. Soc. Jpn. Lett.*, vol. 61, no. 4, pp. 1136–1140, Apr. 1992.

[23] T. H. Kho and A. T. Lin, "Slow-wave electron cyclotron maser," *Phys. Rev. A*, vol. 38, no. 6, pp. 2883–2888, Sept. 1988.

[24] E. Jerby and G. Bekefi, "Cyclotron-maser experiments in a periodic waveguide," *Phys. Rev. E*, vol. 48, pp. 4637–4641, Dec. 1993.

[25] K. P. Maheshwari *et al.*, "Cherenkov-cyclotron resonance interaction in a high-power plasma-filled backward-wave oscillator," *Phys. Rev. A*, vol. 45, pp. 5866–5871, Apr. 1992.

[26] W. W. Destler and S. K. Guharay, Eds., *High Brightness Beam for Advanced Accelerator Applications.* New York: AIP press, 1992.

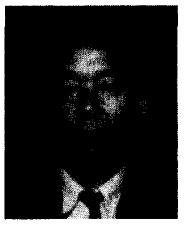

K. Minami was born in Japan in 1938. He received the B.S. (EE) degree at Nagoya Institute of Technology in 1962, the M.S. (EE) degree at the Tokyo Institute of Technology in 1964, and the Ph. D. degree at Nagoya University in 1969.

Since 1986, he has been a Professor in the Electrical Engineering Department of Niigata University, Japan. His research interests include the generation of high-power microwave radiation, and interactions between powerful microwaves and plasmas.

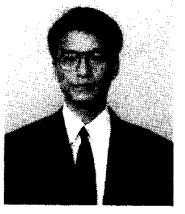

K. Ogura was born in Japan in 1957. He received the B.Sc. degree in physics from Okayama University in 1981, and the M.Sc. and D.Sc. degrees in physics from Kyoto University in 1983 and 1989, respectively.

He is as an Associate Professor in the Electrical and Electronic Engineering Department of Niigata University. His research interests include high-power microwave oscillators and their applications to plasma heating.

Y. Aiba, photograph and biography not available at the time of publication.

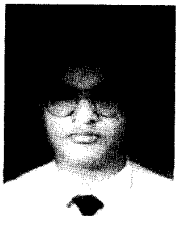

M. R. Amin was born in Rangpur, Bangladesh in 1959. He received the B.Sc. (EEE) degree from the University of Rajshahi in 1984 and the M.Sc. (EEE) degree from Bangladesh University of Engineering and Technology, Dhaka, Bangladesh in 1987. He is pursuing the Ph.D. degree at Niigata University, Japan.

He is now on sabbatical from Bangladesh Institute of Technology, Rajshahi, where he is an Assistant Professor in the Electrical and Electronic Engineering Department. His research interests include theoretical and experimental investigations of high-power microwave devices, and semiconductor power electronic drives.

Mr. Amin is a member of the Institution of Engineers Bangladesh (IEB), and the Physical Society of Japan.

X. D. Zheng was born in Shandong, China in 1962. He received the B.S. and the M.S. degrees in optical engineering from Zhejiang University, Hangzhou, China in 1982 and 1986, respectively. He is pursuing the Ph.D. degree at Niigata University, Japan.

His research interests include theoretical and experimental investigations of high-power microwave devices, and optical measurements.

T. Watanabe was born in Japan in 1941. He received the B.S. degree in physics from the Tokyo Institute of Technology in 1964, and the M.S. and Ph.D. degrees from Nagoya University in 1966 and 1969, respectively.

He is currently with the National Institute for Fusion Science, Nagoya. His research interests include nonlinear plasma dynamics, and a generalized scheme to solve numerically a variety of systems of nonlinear equations.

Y. Carmel (S'66–M'69–SM'90), for a photograph and biography, see page 577 of the October 1994 issue of this TRANSACTIONS.

W. W. Destler (M'84–SM'90–F'92), photograph and biography not available at the time of publication.

V. L. Granatstein (S'59–M'64–Sm'86–F'92), for a photograph and biography, see page 524 of the October 1994 issue of this TRANSACTIONS.